

Unified Accretion Disk Models Around Black Holes and Neutron Stars and Their Spectral Properties

S. K. Chakrabarti

Tata Institute of Fundamental Research, Homi Bhabha Road, Mumbai, 400005, INDIA

Abstract. We review the current understanding of accretion flows around compact objects with a special emphasis on advective disks. We discuss the influence of the centrifugal pressure supported high density region around compact objects (where shocks may also form) on the emitted spectra. We show that the stationary and non-stationary spectral properties (such as, low and high states, transition of states, quasi-periodic oscillations, quiescent and rising phases of X-ray novae, etc.) of both low mass and supermassive black hole candidates could be satisfactorily explained within the framework of the analytical solution of the advective disks without invoking any ad hoc components such as Compton clouds or magnetic corona.

1. Fundamental Properties of Advective Disks

Our understanding of accretion processes around black holes is vastly improved from the analysis of the global solutions which include advection, rotation, viscosity, heating and cooling processes (Chakrabarti, 1990; 1996a; 1996b). Central to the physics of these advective disks is the fact that matter enters through the horizon with a velocity equal to the velocity of light and therefore, the accretion flow must be supersonic and hence sub-Keplerian (Chakrabarti, 1990; 1996bc) in the nearby region. (This was completely ignored by standard disk models of Shakura & Sunyaev, 1973 and Novikov & Thorne, 1973). Thus, every flow must deviate from a (subsonic) Keplerian disk near a black hole. The location from where the deviation occurs as well as the location of the sonic points depend on the heating and cooling effects (i.e., roughly speaking, on viscosity parameter and mass accretion rate). Further, close to a black hole, the infall time scale is much smaller compared with the viscous time scale, and matter plunges into the hole with roughly constant angular momentum. Thus, the centrifugal barrier becomes stronger even for a small angular momentum (the barrier would be infinite for a Newtonian potential) which causes the density of matter to rise rapidly. Matter piled up behind this barrier may or may not produce standing shock waves depending on whether the shock conditions are satisfied. Shock or no shock, the behavior of the enhanced emission of the hotter radiation from the denser region behind the centrifugal barrier appears to be sufficiently relevant to explain the observed spectral properties (stationary or non-stationary) of galactic and extragalactic black hole candidates (Chakrabarti & Titarchuk, 1995; Chakrabarti, 1997).

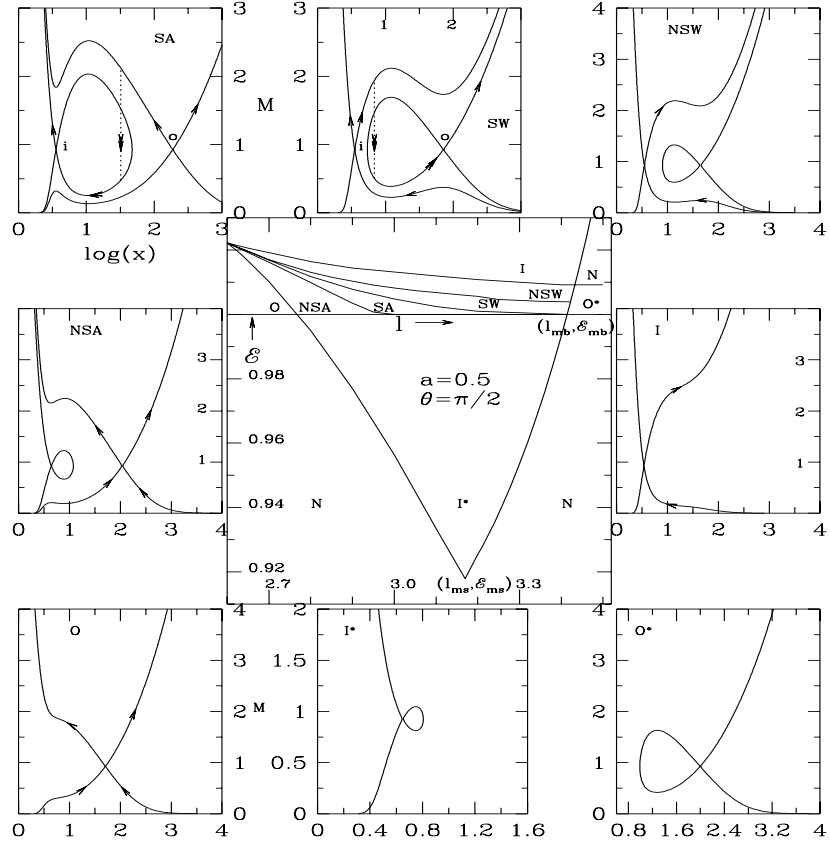


Fig. 1: Classification of the *entire* parameter space (central box) in the energy-angular momentum plane in terms of topological variation of the Kerr black hole accretion ($a = 0.5$ and polytropic index $\gamma = 4/3$). Eight surrounding boxes show the solutions from each independent region of the parameter space. Contours are of constant entropy accretion rate \dot{M} . Vertical arrowed lines correspond to shock transitions.

Fig. 1 shows the classification of the *entire* parameter space according to the types of solutions that are prevalent around a black hole (Chakrabarti, 1996c; see also Chakrabarti, 1989; 1990). In the central box, the parameter space (spanned by specific angular momentum l and specific energy \mathcal{E}) is divided into nine regions marked by N , O , NSA , SA , SW , NSW , I , O^* , I^* . The horizontal line at $\mathcal{E} = 1$ corresponds to the rest mass of the flow. Surrounding this parameter space, various solutions (Mach number $M = v_x/a_s$ vs. logarithmic radial distance x where v_x is the radial velocity and a_s is the sound speed) marked with the same notations (except N) are plotted. The accretion solutions have inward pointing arrows and the wind solutions have outward pointing arrows. The region N has no transonic solution. E and l are the only two parameters required to describe the entire inviscid global solutions. Since E is assumed to be constant, entire energy is advected towards the hole. Thus, these solutions are hot but inefficient radiators very similar to their spherical counterpart (Bondi flow). In the case of neutron star accretion, the subsonic inner boundary condition forces the flow to choose the sub-sonic branch and therefore the energy

must be dissipated at the shock (at x_{s1} or x_{s3} in the notation of Chakrabarti, 1989) outside the neutron star surface (Chakrabarti, 1989; 1990; 1996b) unless the entire flow is subsonic. The solutions from the region ‘O’ has only the outer sonic point. The solutions from the regions *NSA* and *SA* have two ‘X’ type sonic points with the entropy density S_o at the outer sonic point *less* than the entropy density S_i at the inner sonic point. However, flows from *SA* pass through a standing shock since the Rankine-Hugoniot conditions are satisfied. The entropy generated at the shock $S_i - S_o$ is advected towards the black hole to enable the flow to pass through the inner sonic point. Such solutions have been verified by detailed numerical simulations (Chakrabarti & Molteni, 1993; Molteni, Lanzafame & Chakrabarti, 1994; Molteni, Ryu & Chakrabarti, 1996; see also Chakrabarti et al, 1997). Rankine-Hugoniot conditions are not satisfied for flows from the region *NSA*. Numerical simulations show (Ryu, Chakrabarti & Molteni, 1997; Chakrabarti et al. 1997) that flows from this region are very unstable and exhibit periodic changes in emission properties as they constantly try to form stationary shocks, but fail to do so. The frequency and amplitude of modulation (10-50%) of emitted X-rays have properties similar to Quasi-Periodic Oscillations observed in black hole candidates (Dotani, 1991). In galactic black holes, these frequencies are around 1Hz (exact number depends on shock location, i.e., l , \mathcal{E} parameters) but for extragalactic systems the time scale could range from a few hours to a few days depending on the central mass ($T_{QPO} \propto M_{BH}$). Numerous cases of QPOs are reported in the literature (e.g., Dotani, 1991; Halpern & Marshall, 1996; Papadakis & Lawrence, 1995). In presence of cooling effects, otherwise stationary shocks from *SA* also oscillate with frequency and amplitude modulations comparable to those of QPOs *provided* the cooling timescale is roughly comparable to the infall timescale in the post-shock region (Molteni, Sponholz & Chakrabarti, 1996). KiloHertz oscillations on neutron stars (van der Klis, this volume) are also possible when the shock at x_{s1} form. The solutions from the regions *SW* and *NSW* are very similar to those from *SA* and *NSA*. However, $S_o \geq S_i$ in these cases. Shocks can form only in winds from the region *SW*. Shock conditions are not satisfied in winds from the region *NSW*. This makes the *NSW* flows unstable as well. A flow from region *I* has only the inner sonic point and thus can form shocks (which require the presence of two saddle type sonic points) if the inflow is already supersonic due to some other physical processes (as in a wind-fed system). Each solution from regions I^* and O^* has two sonic points (one ‘X’ and one ‘O’) only and neither produces complete and global solution. The region I^* has an inner sonic point but the solution does not extend subsonically to a large distance. The region O^* has an outer sonic point, but the solution does not extend supersonically to the horizon! When a significant viscosity is added, the closed topology of I^* opens up and then the flow joins with a cool Keplerian disk (C90ab; C96) which has $\mathcal{E} < 1$. These special solutions of viscous transonic flows should not have shock waves. However, hot flows deviating from a Keplerian disk or sub-Keplerian companion winds, or flows away from an equatorial plane (Chakrabarti, 1996d) or, cool flows subsequently preheated by magnetic flares or irradiation can have $\mathcal{E} > 1$ and therefore standing shock waves. Note that in order to have standing shocks, one does not require any large angular momentum. Indeed, in most of the cases, the flow need to have $l \ll l_{ms}$, the marginally stable value (Fig. 1). Although a flow with polytropic index $\gamma < 1.5$ does not have shocks,

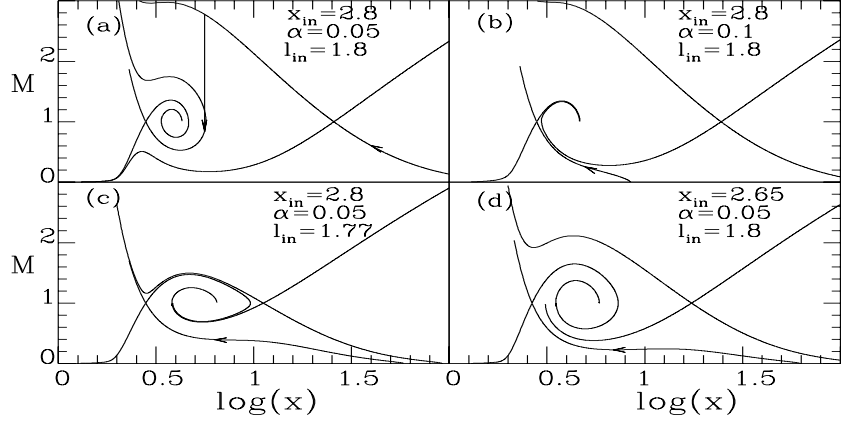


Fig. 2: Change in solution topology of a viscous flow as the three parameters are varied (Chakrabarti, 1990). In (a), after deviating from a hot Keplerian disk the flow can pass through the outer sonic point, shock and the inner sonic point (shown in arrows), while in (b-d) the stable flow can pass through the inner sonic point after it deviates from a Keplerian disk. Density and velocity distribution in the flow close to the black hole remain roughly the same in all these cases. Distance x is measured in units of x_g .

the stationary observational properties, which depend only on the enhanced emission from the region behind of centrifugal barrier, are not affected.

When viscosity is added, the closed topologies shown in Fig. 1 open up as the ‘O’ type sonic points become spiral or nodal type. Singularly important in this context is the non-trivial change in topology when each of the three free parameters are changed (Chakrabarti, 1990). In the context of viscous isothermal flows (These discussions are valid for a general flow as well, see, Chakrabarti, 1996ab.) these free parameters can be chosen to be inner sonic point x_{in} (this replaces the specific energy parameter), the angular momentum on the horizon l_{in} and the viscosity parameter α . Temperature of the disk is computed self-consistently from these parameters. Fig. 2 shows that transition to topology in (b-d) from topology (a) can take place either by increase in viscosity or decrease x_{in} or l_{in} . In (a), shocks are still possible, while in (b-d), shocks do not form as the flow enters into the hole through the inner sonic point straight away from a Keplerian disk, but the density variation and emission properties remain similar to that of a shocked flow. In (b), Keplerian disk is extended close to the horizon, while in (a) the deviation takes place farther outside of the outer sonic point. Thus, for instance, if there is a vertical variation of viscosity in a Keplerian disk very far away from a black hole, it is possible that different layers would deviate from a Keplerian disk at different radial distance, and a sub-Keplerian flow (with or without a shock) would surround a Keplerian disk as the flow approaches the compact object. The sub-Keplerian flow could also be contributed by companion winds in wind-fed systems. This two component advective flow (TCAF) Model (Chakrabarti & Titarchuk, 1995), for the first time, obviates the need of having any ad hoc Compton cloud or magnetic coronae required in the past to explain the power law components of black hole spectra. Here, one computes the properties of the so called ‘Compton

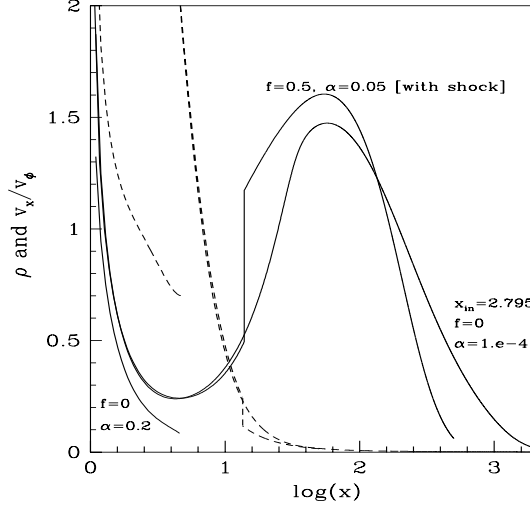


Fig. 3: Ratios v_x/v_ϕ (solid) and densities (dashed) of three illustrative solutions of the advective flows (Chakrabarti, 1996b). Note that the centrifugal barrier close to the hole makes all the three solutions to behave similarly in the region $2 \lesssim x \lesssim 10$, emission from which strongly determines the spectral properties of the hole. In a strongly shocked flow the variations occur in a shorter length scale while in a weakly shocked or shock-free flows the variations occur in an extended region.

cloud’ self-consistently since it is a part of the inflow itself. Extensive numerical simulations (Chakrabarti & Molteni, 1995; Chakrabarti et al. 1997) of viscous advective flows verify these analytical findings.

In Fig. 3, we show a common property of advective flows which ‘feel’ centrifugal barrier close to the hole. We plot the ratio of radial to azimuthal velocities (solid curves) as well as the density (dashed curves) of the flow (in arbitrary units) as functions of the radial distance of three illustrative examples of solutions (Chakrabarti, 1996b). Here, $f = (Q_+ - Q_-)/Q_+$ is chosen to be constant throughout the flow for simplicity. For a given angular momentum of the flow at the horizon, solutions without shocks (marked with $\alpha = 1.e - 4$ and $\alpha = 0.2$) and that with a shock ($\alpha = 0.05$) have similar properties close to a black hole, namely, all have $v_x/v_\phi \ll 1$ around $2 \lesssim x \lesssim 10$. Density and velocity distributions in the postshock region are similar to those in the subsonic shock-free flow. Thus, in some sense, all the solutions have ‘shocks’ behind the centrifugal barrier. Only the length scales in which the quantities change vary. Hence, *qualitative* spectral properties of the TCAF Model does not seriously depend on whether the shocks actually form in either or both of the Keplerian (which also becomes sub-Keplerian close to the hole) and the sub-Keplerian components. However, spectral properties *do depend* upon whether the accretion flow is of single component (such as one Keplerian flow becoming entirely sub-Keplerian close to the hole) or two components (where the original Keplerian disk plus companion winds are segregated into Keplerian and sub-Keplerian components very far away before being mixed into a single sub-Keplerian component near the hole). This will be demonstrated below.

2. Observational Properties of Two Component Advective Flows.

Based upon the theoretical unstanding of the properties of Advective flows, Chakrabarti & Titarchuk (1995) pointed out that the accretion on most compact objects may be taking place in two components: one is of higher viscosity, predominantly Keplerian (Disk Component) and is extended till around $x_K = 10x_g$ if the accretion rate is high enough to keep it thermally and viscously stable, otherwise x_K could be higher (see also, Ebisawa, Titarchuk & Chakrabarti, 1996). Keplerian region of the disk component supplies soft photons. The other component (Halo Component) is predominantly sub-Keplerian (which is originated from the Keplerian disk far away and is contributed by companion winds, if present, in the case of a galactic black hole and by winds from numerous stars in the case of a supermassive black hole.) This component radiates inefficiently and therefore is hot (\sim virial temperature) and together with $x < x_K$ of the disk component they supply hot electrons which in turn energize intercepted soft photons to produce hard component. The extent to which electrons cool is determined by the accretion rates in these two components. At least three important variations of this Model is recognized: TCAFM1– In this case, the halo component forms a strong shock behind the centrifugal barrier: $x_s \sim 10x_g$ and puffs up and mixes up with the disk component at $x < x_s$. TCAFM2– The halo component does not form a shock or forms only a weak shock but still feels the centrifugal barrier as in TCAFM1. TCAFM3– The halo component is completely devoid of angular momentum. The disk component deviates from a Keplerian disk at x_K . For $x < x_K$ these components mix as before. In this case, the absence of centrifugal barrier reduces the optical depth of the region $x < x_K$ and it is easy to cool this region even at a low disk rate. A corollary of these Models is a single component model SCAFM, where the sub-Keplerian component rate is so low that it is practically non-existent. In SCAFM, soft photons of the Keplerian region may or may not cool the hot electrons of its own sub-Keplerian region (for $x < x_K$) very effectively depending on x_K and the spectra remains soft in most of the parameter space. Also, in this case, the hard and soft components are always anticorrelated while observations suggest that very often they behave independently. In Chakrabarti & Titarchuk (1995), TCAFM1 is extensively studied while other possibilities are also mentioned (see also Ebisawa et al. 1996). More detailed study of these models are in Chakrabarti (1997). Fig. 4a schematically shows the possible flow model based on the analytical considerations. Note that this generalized disk of the 1990s (and hopefully of the future) is really a natural combination of purely advecting Bondi flow of the 1950s and purely rotating Keplerian disks of the 1970s. In Fig. 4b we show the basic difference in the soft state spectra of neutron stars and black holes. In the soft state, the disk rate is large and emitted soft photons completely cool the inner quasi-spherical sub-Keplerian region. The inner boundary property on the horizon of a black hole causes the cool (but rushing with velocity comparable to the velocity of light) electrons to Comptonize a fraction of these soft photons due to direct momentum transfer (as opposed to random momentum transfer in thermal Comptonization) and produces a weak hard tail component with photon index $\sim 2.5 - 3$. While on a neutron star such a hard component must be missing since the flow has to slow down on the inner boundary. Just for completeness, a naked singularity (NSing, with inner boundary at $x \sim 0$)

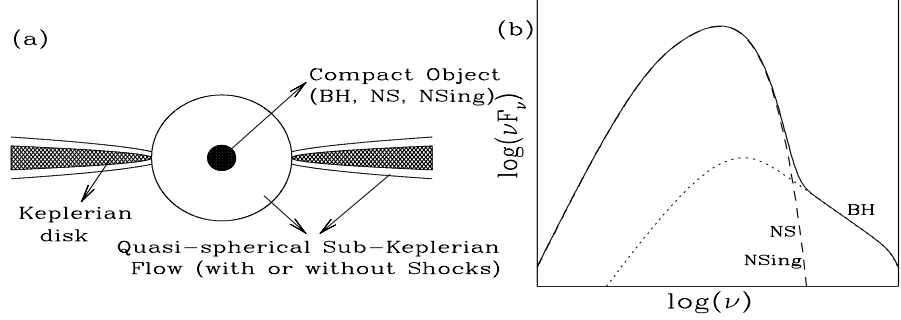


Fig. 4: (a) Schematic diagram of the two component advective disk model. Keplerian disk component which eventually becomes sub-Keplerian close to a compact object is flanked by a sub-Keplerian halo component which is originated from the Keplerian disk farther out and possibly contributed by winds of the companion or nearby stars. (b) Soft states of neutron stars (NS), black holes (BH) and naked singularities (NSing) are distinguished by the presence or absence of the weak hard tail component possibly due to bulk motion Comptonization (Chakrabarti & Titarchuk, 1995).

also should not have this weak hard tail since extremely dense advecting matter close to the singularity would carry all such hard photons inwards. This feature is because the absorbing boundary is at $x = 0$ (Chakrabarti & Titarchuk, 1995).

Fig. 5 shows examples of spectral transitions in black hole candidates in all the three models described above. We choose here $M_{BH}^* = 1M_\odot$, which after correction due to spectral hardening (Shimura & Takahara, 1995), corresponds to a mass of $M_{BH} \sim 3.6M_\odot$. All the rates are in units of Eddington rate. In Fig. 5(a), we consider three disk rates $\dot{m}_d = 0.3, 0.05, 0.0005$ but the same halo rate $\dot{m}_h = 1$. Solid, long-dashed and short-dashed curves are for strong shock Model (TCAFM1), weak or no-shock Model (TCAFM2) and zero angular momentum halo Model (TCAFM3). For a set of (\dot{m}_d, \dot{m}_h) , the spectrum is hardest for TCAFM1 and softest for (TCAFM3). This is expected since the emission region has the highest density when shocks are stronger. SCAFM always produces soft states for these parameters. In Fig. 5(b), we show the comparison of energy spectral index α (where $F[E] \sim E^{-\alpha}$) for these models as functions of \dot{m}_d . In all these models, spectra becomes soft even when the disk rate is much below Eddington rate. In the case of supermassive black holes, the behavior is very similar as the electron temperature of the sub-Keplerian region is very insensitive to the central mass ($T_e \propto M_{BH}^{0.04}$). At high accretion rate, the bulk motion Comptonization produces weaker hard tail (Chakrabarti & Titarchuk, 1995). Its behavior is independent of any model and depends mainly on the optical depth in the last few Schwarzschild radii outside the horizon. In the long dashed region of the convergent flow curve, both power laws due to thermal and bulk motion Comptonizations are expected in the observed spectra. In Fig. 5(c), the dependence of the spectra on the location where the flow deviates from a Keplerian disk (x_K) is shown using TCAFM3. Fig. 5(d) shows the corresponding variation of the spectral index. As described in Chakrabarti & Titarchuk (1995) and Chakrabarti (1996b), this variation of x_K could be simply due to the viscosity variation in the flow (see, Fig. 2 above) and therefore such

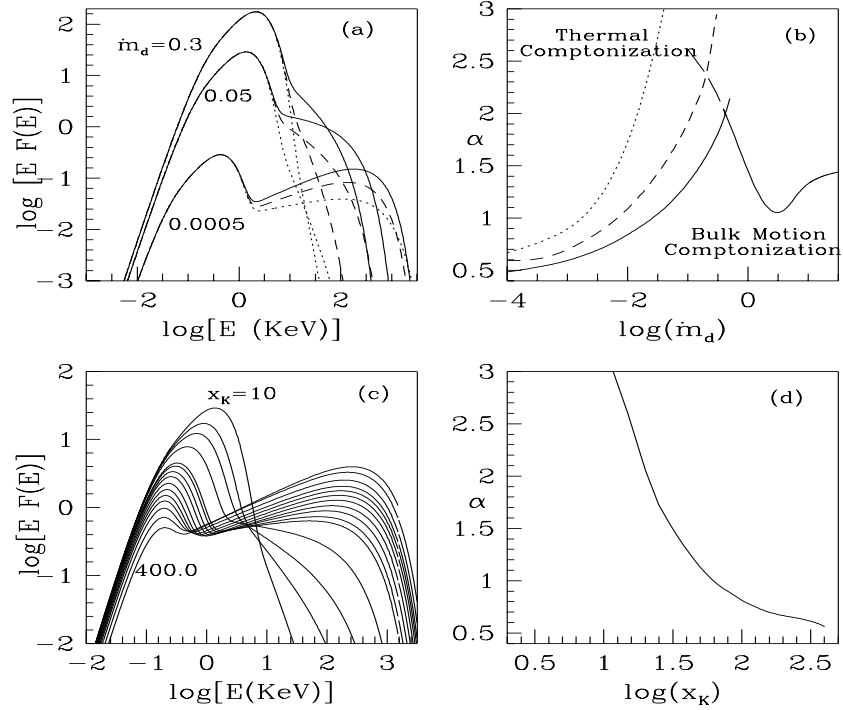


Fig. 5: Model dependence of spectral properties. (a) Solid, long-dashed and short-dashed curves are for TCAFM1, TCAFM2 and TCAFM3 respectively. (b) Spectral indices of the corresponding models as functions of \dot{m}_d are drawn. (c) Result of TCAFM3 ($\dot{m}_d = 0.05$, $\dot{m}_h = 1.0$). Spectrum changes from hard state to soft state as the Keplerian disk approaches the black hole due to increase in α and \dot{m}_d (as probably in the rising phase of a novae outburst). (d) Changes in spectral index with x_K .

variation in the spectra is expected in viscous time scale, specially during the rising phase of a novae outburst which is presumably induced by an enhancement in viscosity (see, Cannizzo 1993 and references therein) at the outer edge of the Keplerian disk. Figs. 5(c-d) were drawn for $\dot{m}_d = 0.05$ and $\dot{m}_h = 1.0$. Indeed, rising light curves (Fig. 6c-d) derived from this consideration is remarkably similar to what is observed. In reality both rates must change. Such a transition is best understood by a numerical simulation of viscous advective flow together with radiative transfer (Chakrabarti et al. in preparation).

It is interesting to compare the results of TCAF Models presented above with some of the observations of black hole candidates. In Fig. 6 spectral evolutions of two well known X-ray novae are roughly fitted with TCAFM1. The spectral data of GS2000+25 are taken from Tanaka (1991) and those of GS1124-68 are from Ebisawa (private communication; Ebisawa et al., 1994). For simplicity and to highlight the similarity between these two objects, all the parameters have been kept fixed (with $x_s = 10x_g$, $x_g = 2GM_{BH}/c^2$, and Schwarzschild black hole of mass $1M_\odot$ which after correction due to spectral hardening corresponds to $3.6M_\odot$) *except* for the rates \dot{m}_d and \dot{m}_h . Figs. 6(a-b) show these fits. From the derived pair of rates (\dot{m}_d , \dot{m}_h) the intermediate rates

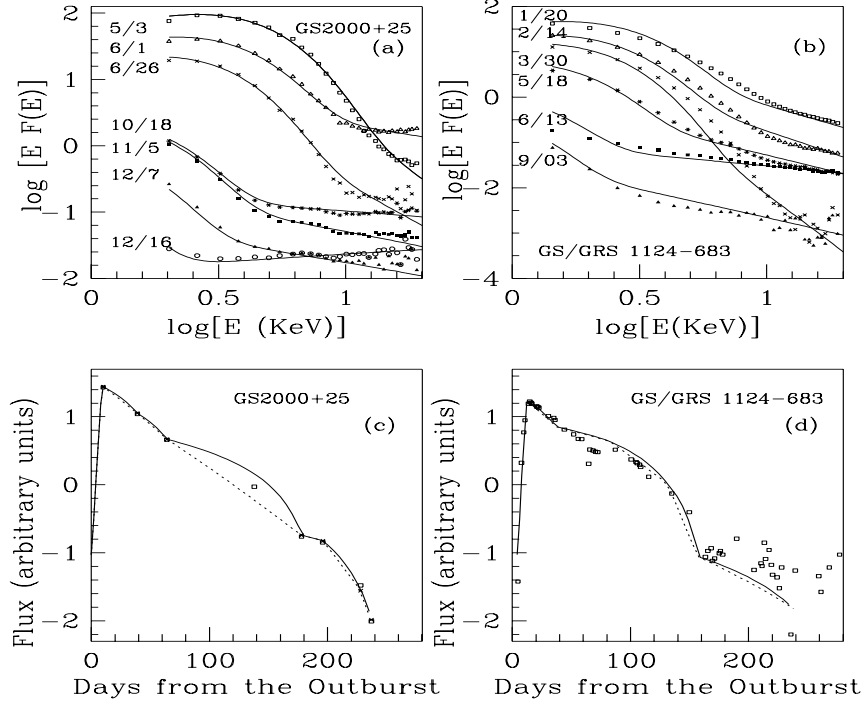


Fig. 6: Rough fits of evolution of two X-ray novae spectra using two component advective flow model (TCAFM1) and comparison of derived light curves with the observed light curves. See text for details.

are interpolated and the resulting light curves (1-20keV) are shown in Figs. 6(c-d). Solid and dotted light curves are drawn using linear-linear and linear-log interpolations of \dot{m}_d respectively. In Fig. 6(c), squared points are obtained from the actual spectra while crosses are obtained from the fit in Fig. 6(a). In Fig. 6(d), the squares are from ASM light curve of Ginga (Kitamoto, private communication; Kitamoto et al. 1992). The general features of the light curves are clearly reproduced, including the bumps after 50-70 days and another one after 200 days of outburst. Both show a decay time scale of ~ 33 days. The bump around 50-70d shows that the decay of disk accretion rate is not exponential, but more like linear although after around 200 days the disk rate dropped to the point where the exponential decay would have brought it. The rising light curves in both the cases were computed in two different ways and the results were similar. In one case (using TCAFM1), the \dot{m}_d was increased from a quiescent state with an e-folding time of ~ 2 days, while in the other case (using TCAFM3), the x_K was reduced exponentially at a similar rate.

Spectral behavior in above systems and other systems (see, e.g., Ebisawa et al. 1994 for LMC X-3, Crary et al. 1996 for Cyg X-1), universal presence of the weak hard tail in soft states, diverse observations such as quiescent states to rising phases of black hole candidate novae, soft to hard transitions, pivoting property of the spectra, quasi-periodic oscillations (including observed large amplitude modulations) are naturally explained by TCAF models without invoking

any additional unknown components. Though we did not include magnetic fields explicitly, existence of small fields as generated by say, Balbus-Hawley instability (this volume), cannot affect our results. Finally, we wish to point out that even the jets and outflows are found to be formed more easily from a sub-Keplerian flow (Chakrabarti & Bhaskaran, 1992).

Acknowledgments. The author acknowledges helpful discussions with Drs. Ken Ebisawa, Sunji Kitamoto and S. Nan Zhang.

References

- Cannizzo, J. 1993 in *Accretion Disks in Compact Stellar Systems* J. C. Wheeler, World Scientific: Singapore
- Chakrabarti, S.K. 1989, *ApJ*, 347, 365
- Chakrabarti, S.K. 1990, *Theory of Transonic Astrophysical Flows*, World Scientific: Singapore
- Chakrabarti, S.K. 1996a, *Phys. Rep.*, 266, 229
- Chakrabarti, S.K. 1996b, *ApJ* 464, 664
- Chakrabarti, S.K. 1996c, *MNRAS*(Nov. 1st)
- Chakrabarti, S.K. 1996d, *ApJ*(Nov. 1st)
- Chakrabarti, S.K. 1997, *ApJ* submitted
- Chakrabarti, S.K. & Bhaskaran, P. 1992, *MNRAS*, 255, 255
- Chakrabarti, S.K. et al. 1997, this volume
- Chakrabarti, S.K., & Molteni, D. 1993, *ApJ*, 417, 671
- Chakrabarti, S.K. & Molteni, D. 1995, *MNRAS*, 272, 80
- Chakrabarti, S.K. & Titarchuk, L. G. 1995, *ApJ*, 455, 623
- Crary, D.J. et al. *ApJ*, 1996, 462, 71L
- Dotani, Y. 1992 in *Frontiers in X-ray Astronomy*, Tokyo: Universal Academy Press, Y. Tanaka & K. Koyama 152
- Ebisawa, K., Titarchuk, L. & Chakrabarti, S. K., 1996, *PASJ*, 48, 1
- Ebisawa, K. et al. 1994, *PASJ*, 46, 375
- Halpern, J. & Marshall, H. L. 1996, *ApJ*, 464, 760
- Kitamoto, S. et al. 1992, *ApJ*, 394, 609
- Molteni, D., Lanzafame, G., & Chakrabarti, S. K. 1994, *ApJ*, 425, 161
- Molteni, D., Sponholz, H. & Chakrabarti, S. K. 1996, *ApJ*, 457, 805
- Molteni, D., Ryu, D. & Chakrabarti, S. K. 1996, *ApJ*, (Oct 10th)
- Novikov, I. & Thorne, K. S. 1973, in *Black Holes*, C. DeWitt and B. DeWitt, Gordon and Breach: New York
- Papadakis, I. E. & Lawrence, A. 1995, *MNRAS*, 272, 161
- Shakura, N. I. & Sunyaev, R. A. 1973, *A&A*, 24, 337
- Shimura, T. & Takahara, F. 1995, *ApJ*, 445, 780
- Ryu, D., Chakrabarti, S.K. & Molteni, D. 1997, *ApJ*, (Jan. 1st)
- Tanaka, Y. 1991 in *Iron Line Diagnostics in X-ray Sources* A. Treves et al. Springer-Varlag: Heidelberg

To appear in: 'Accretion Phenomena and Related Outflows', proceedings of 163rd IAU Symposium, July-1996, Eds. D. Wickramasinghe, L. Ferrario and G. Bicknell.

Author's address from November 26th, 1996:

Prof. S.K. Chakrabarti
S.N. Bose National Center for Basic Sciences
JD Block, Sector -III, Salt Lake
Calcutta 700091, INDIA

e-mail: chakraba@bose.ernet.in OR chakraba@tifrc2.tifr.res.in